EFFECT OF ELASTIC BENDING RESTRAINTS ON THE BEHAVIOR OF THIN GLASS PLATES

Kamel Sayed Kandil
Civil Engineering Department, Faculty of Engineering,
Menufiya University, Shebin El-Kom, Egypt.

ABSTRACT

von Karman equations are used to represent the behavior of thin rectangular glass plates subjected to lateral pressures. A previously reported model that used a finite difference method solved the glass plate problem assuming the edges to be resting on elastic transitional springs acting in the out-of-plane direction. The plate edges were assumed to be free to rotate in the lateral direction. Here, this model is modified to include condition where the plate is also elastically restrained against rotation along its boundaries in the lateral direction. It is found that these bending restraints have a significant effect on the behavior of the plate and that the number of iterations required in the solution process are reduced by using this condition.

INTRODUCTION

The pioneers of the analysis of thin plates were Cauchy, Poisson, Navier, and Kirchoff [1]. The research done by these pioneers as early as the 1800s is significant and most of the analysis done by them is still used in engineering analysis.

When the lateral displacement of the plate increases more than its thickness, the linear theories are not useful. Membrane stresses are developed in the plate in addition to bending stresses. To account for these membrane stresses, a nonlinear plate theory was developed in 1910 by von Karman [1] for the analysis of thin plates subjected to lateral pressures. Since the resulting field equations are nonlinear, there are no closed form solutions available to solve these equations. Al-Tayyib [2] and Tsai and Stewart [3] used the finite element method to solve this problem. Vallabhan [4] solved the nonlinear flat plate problem using a finite difference oriented method that employs an efficient iterative technique.

The investigators listed above, used simply supported boundary conditions in the solution of the problem. Wang [5] presented a model where the plate edges were assumed to be resting on elastic transitional springs acting in the out-of-plane direction. The plate edges were assumed to be free to rotate in the lateral direction. He concluded that the effect of these springs is small and localized at the plate corners. In reality, glass plates are supported by neoprene gaskets or sealants that offer not only elastic out-of-plane restraints but also, elastic bending restraints to the plate edges (see Figure (1)). Small bending restraints on the plate edges can affect the magnitudes and locations of maximum stresses in the glass plate. Thus, consideration of the properties of these elastic supports is important to the analysis of glass plates.

This paper summarizes the development of a finite difference model for thin rectangular glass plates that are supported by elastic gaskets or sealants on their boundaries. Elastic out-of-plane and bending restraints are assumed to be offered by these supports.

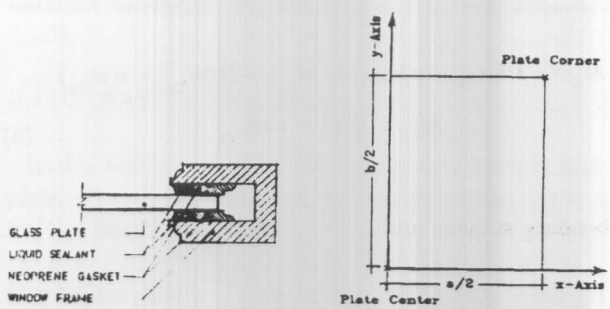

Figure 1. a) Window Glass Plate Fastened in a Rigid Framing System using Rubber-Like Gaskets. b) Sketch Showing One Quarter of the Plate.

THE MATHEMATICAL MODEL

The governing differential equations and boundary conditions for a thin rectangular glass plate subjected to lateral pressure and resting on elastic supports that offer out-of-plane and bending restraints are as follows [1] [6]:

$$D\nabla^4 w = q + t\,L(w,F) \tag{1}$$

and

$$\nabla^4 F = -\frac{E}{2} L(w,w) \tag{2}$$

where:

D = $Et^3/12(1-\upsilon^2)$ = flexural rigidity of the plate;
w = the lateral displacement of the middle

surface of the plate;
F = Airy's stress function;
q = lateral pressure;
t = thickness of plate;
E = Young's modules of elasticity of the plate;
ν = Poisson's ratio;
∇^4 = biharmonic operator;

and $L(w, F) = (w_{,xx}F_{,yy} - 2w_{,xy}F_{,xy} + w_{,yy}F_{,xx})$

From this expression $L(w,w)$ can be obtained by substituting w for F. The subscript "comma" notation represents differentiation with respect to the variables following it. The Airy's stress function F represents the membrane stresses [7] such that:

$$\sigma_x^m = F_{,yy} \; ; \quad \sigma_y^m = F_{,xx} \; ; \quad \tau_{xy}^m = -F_{,xy} \tag{3}$$

The moment resultants per unit length of the coordinate axes are given by M_x, M_y, and M_{xy} and are expressed as:

$$M_x = -D(w_{,xx} + \nu w_{,yy}) \; ; \quad M_y = -D(w_{,yy} + \nu w_{,xx})$$
$$M_{xy} = D(1-\nu)w_{,xy} \tag{4}$$

The bending stresses are:

$$\sigma_x^b = \pm 6\frac{M_x}{t^2} \tag{5}$$

$$\sigma_y^b = \pm 6\frac{M_y}{t^2} \tag{6}$$

$$\tau_{xy}^b = \pm 6\frac{M_{xy}}{t^2} \tag{7}$$

The boundary conditions for a plate resting on supports, which offer elastic out-of-plane and moment restraints are as follows (only one quarter of the plate is considered because of symmetry - see Figure (1-b)):

At x = a/2:

$$\tau_{xy}^m = -F_{,xy} = 0 \tag{8}$$

$$\sigma_x^m = F_{,yy} = 0 \tag{9}$$

$$D[w_{,xxx} + (2-\nu)w_{,xyy}] = wK_v \tag{10}$$

and $$D(w_{,xx} + \nu w_{,yy}) = w_{,x}K_m \tag{11}$$

At x = 0:

$$w_{,x} = 0 \quad \text{(symmetry)} \tag{12}$$

At y = b/2:

$$\tau_{xy}^m = -F_{,xy} = 0 \tag{13}$$

$$\sigma_y^m = F_{,xx} = 0 \tag{14}$$

$$D[w_{,yyy} + (2-\nu)w_{,yxx}] = wK_v \tag{15}$$

and $$D(w_{,yy} + \nu w_{,xx}) = w_{,y}K_m \tag{16}$$

At y = 0:

$$w_{,y} = 0 \quad \text{(symmetry)} \tag{17}$$

where

K_v = Spring constant of the elastic yielding support.
K_m = Spring constant of the elastic bending restraints.

Equs. (10) and (15) represent the conditions of elastically yielding supports. Equs. (11) and (16) represent the conditions of elastic moment restraints.

SOLUTION TECHNIQUE

The basic methodology used here is an extension to the model developed by Wang [5]. The major development in this model lies in the incorporation of the elastic bending restraints along the elastically supported edges.

The finite difference operator ∇^4, which applies to all interior nodes that are at least two nodes away from the boundary, is shown for convenience of the readers in Appendix I, Figure (9). For any node close to or on the boundary, all boundary conditions are incorporated along with the main field equation. The molecules for these nodes are developed using two fictitious nodes outside the domain of the plate. For the molecules near and on the boundary, the boundary conditions indicated by Equs. (11) and (16) are enforced. For all the molecules on the boundary, an additional boundary condition is enforced: The Kirchoff shear forces are set equal to the elastic yielding support constant K_v times the deflection w at that node. The

molecules for all points close to or on the boundary are shown in Appendix I, Figures (9) to (17).

Using these finite difference equations the two nonlinear plate equations given in Equs. (1) and (2), are replaced by two sets of algebraic equations: one for the lateral defections and the other for the Airy's stress functions. Both of them are defined at discrete points in the domain of the plate. Consequently, the problem of solving the nonlinear differential equations have been transformed into the solution of two sets of nonlinear simultaneous equations as shown:

$$[A]\{w\} = \{q\} + \{f_1(w, F)\} \tag{18}$$

and

$$[B]\{F\} = \{f_2(w)\} \tag{19}$$

in which matrices $[A]$ and $[B]$ = equivalent biharmonic operators; $\{w\}$, $\{q\}$, and $\{F\}$ = vectors representing the displacements, loads, and values of the stress function F at the discrete points, and $\{f_1\}$ and $\{f_2\}$ are nonlinear functions representing part of the right hand side of Equ. (1) and the right hand side of Equ. (2); respectively. Since the biharmonic operator is linear, both equations on the left hand side are linear, and represented by matrices $[A]$ and $[B]$. Both matrices are symmetric and positive definite, and so they are formed in the computer code as half banded matrices for computational efficiency. An efficient iterative algorithm as given by Vallabhan [4] is employed here.

ITERATIVE SCHEME

Using values of $\{w^i\}$ and $\{F^i\}$ obtained from the ith iteration, the function f_1 is calculated numerically. For the $(i+1)^{th}$ iteration

$$[A]\{w^{i+1}\} = \{q\} + \{f_1(w^i, F^i)\} = \{R_1\} \tag{20}$$

Solving for $\{w^{i+1}\}$ and substituting in Equ. (21) for f_2 we have:

$$[B]\{F^{i+1}\} = \{f_2(w^{i+1})\} = \{R_2\} \tag{21}$$

and solving Equ. (21), we get $\{F^{i+1}\}$. It is experienced that the aforementioned iterative scheme will not converge as deflections become large. In order to obtain converging solution, both the deflection and the stress function were interpolated using two interpolating parameters α and β, such that

$$\tilde{w}^{i+1} = (1-\alpha)\tilde{w}^i + \alpha w^{i+1} \tag{22}$$

and

$$\tilde{F}^{i+1} = (1-\beta)F^i + \beta F^{i+1} \tag{23}$$

The under relaxation parameter α varies nonlinearly with (w_{max}/t) while β is kept equal to 1/2. w_{max} = value of the displacement of the center of plate. Thus, the equations to be solved for the $(i+1)^{th}$ iteration are rewritten as follows:

$$[A]\{w^{i+1}\} = \{q\} + \{f_1(\tilde{w}^i, \tilde{F}^i)\} \; ; \tag{24}$$

and

$$[B]\{F^{i+1}\} = \{f_2(\tilde{w}^{i+1})\} \tag{25}$$

The iteration is continued until the solution converges to a final value for each increment of load such that, the error in w for the $(i+1)^{th}$ iteration

$$\varepsilon^{i+1} = \frac{\sum_{j=1}^{N} \| w_j^{i+1} - w_j^i \|}{N} \leq \gamma (w_{max})^{i+1} \tag{26}$$

in which N = the total number of nodes in the grid, where γ is a prescribed small positive number to represent the iteration tolerance. In this analysis γ was kept equal to 0.001.

ILLUSTRATIVE EXAMPLES

In this section we show the results of a sample thin glass plate. The dimensions and properties of the plate are as follows (see Figure (2)):

Size of the plate	$a = b = 60$ *in* (152.4 *cm*);
Thickness of plate	$t = 0.1875$ *in* (0.48 *cm*);
Modules of elasticity	$E = 10^7$ *psi* (6.9×10^7 *kPa*);
Poisson's ratio	$\upsilon = 0.22$

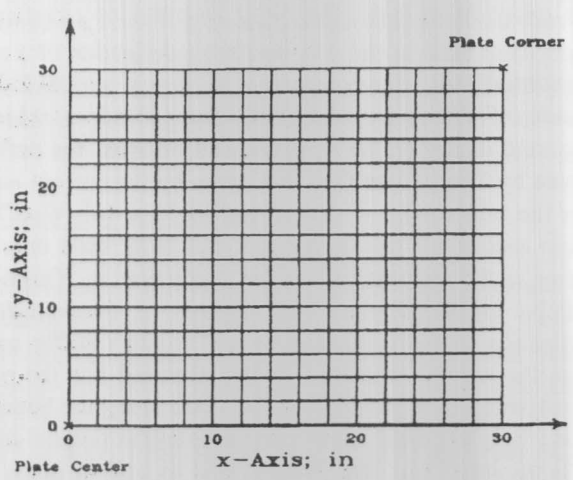

Figure 2. Sketch Showing Plate Axes and Finite Difference Grid; (Only One Quarter of the Plate is Shown).

The glass plate was subjected to a uniform lateral pressure up to 0.64 *psi* (4.41 *kPa*) and was analyzed using grid size 15x15 for a quarter plate. A spring constant $K_v = 10^{20}$ *psi* (6.9×10^{17} *MPa*) was used throughout this study. This value of K_v was shown by Wang [5] to represent rigid supports regarding out-of-plane deflection. Maximum deflections at the plate center are plotted against the bending restraint constant K_m as shown in Figure (3).

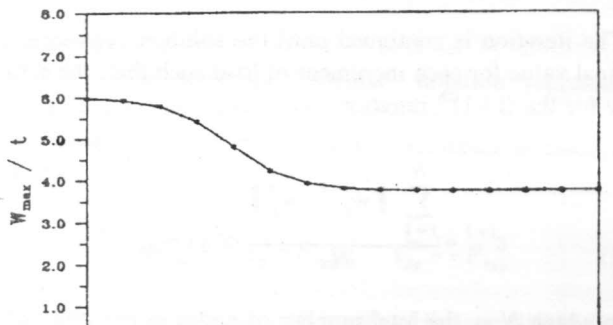

Figure 3. Effect of Bending Restraint Constant; K_m on Maximum (Central) Deflection; (1 *lb* = 4.45 *N*).

The maximum deflection of the plate evidently depends upon the magnitude of K_m. It is seen that increasing K_m decreases the maximum deflection. But, when K_m is greater than 10^5 *lb/rad* (4.45×10^5 *N/rad*) the plate behaves as fixed supported plate.

Figure (4) shows the variation of maximum (central) deflection against the applied loads for different values of K_m. It shown that for a value of $K_m = 10^3$ *lb/rad* (4.45×10^3 *N/rad*) the deflection of the plate at $q = 0.64$ *psi* (4.41 *kPa*) reduces to 80% of the corresponding deflection of a simply supported plate. For comparison the figure also includes the results of Way for a plate with clamped edges, which are reported in Ref [1, pp 421]. As can be seen, the deflection given by Way is less than that given by the current analysis for the case of $K_m = 10^8$ *lb/rad* (4.45×10^8 *N/rad*). The main reason for this is the fact that Way used only three terms in his expression for the deflection *w*. This limited number of terms gives less degrees of freedom for the deflection of the plate, and hence, yields a stiffer solution than the current solution. He also assumed that the plate is constrained from pulling-in in its plane along the boundaries (*i.e.*, fully clamped edges); however in the present analysis it is assumed that the plate is free to pull-in in its plane along the boundaries.

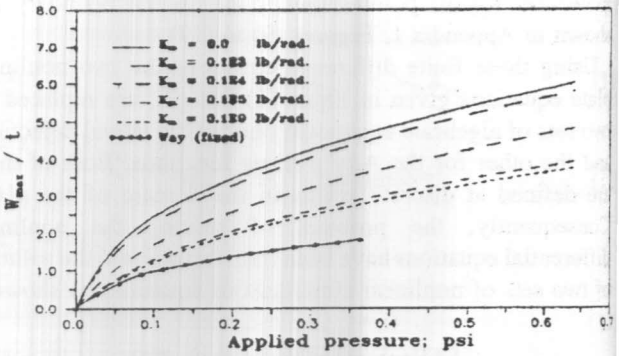

Figure 4. Maximum (Central) Deflection Versus Appli Pressure for Different Values of K_m; (1 *psi* = 6.9*kPa*; 1 *lb* = 4.45 *N*).

Figure (5) illustrates the deflection of the plate along i central line (see Figure (2)) for different values of K_m a at a load pressure = 0.64 *psi* (4.41 *kPa*). As can be see from this figure, the slope of the deflection curve at the pla edge decreases with the increase of K_m. At $K_m = 10^4$ *lb/r* (4.45×10^4 *N/rad*) the slope approaches that of a fix supported plate. The curve shows clearly the reduction of t plate deflection with the increase of K_m.

Figure (6) shows the variation of the edge moment alon the plate edge at $q = 0.64$ *psi* (4.41 *kPa*) with the increas in the value of K_m. As can be seen from this figure t degree of nonlinearty in the edge moment along the pla edge increases with the increase of K_m. It is also seen th for higher values of K_m, although the edge moment increas with the increase of K_m at most of the plate edge it decreas when we approach the plate corner.

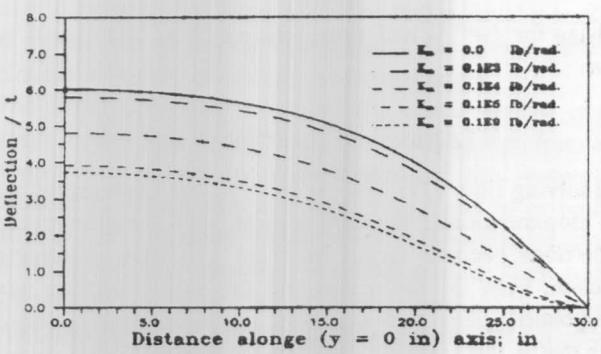

Figure 5. Effect of K_m on plate deflection at 0.64 p pressure; (1 *lb* = 4.45 *N*; 1 *in* = 2.54 *cm*).

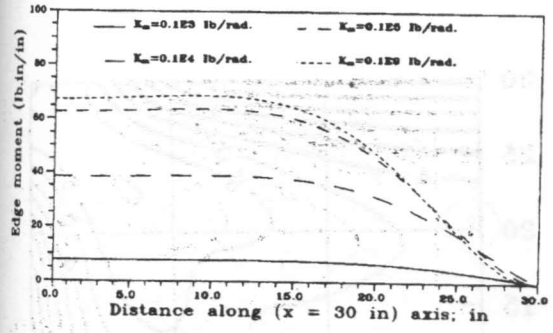

Figure 6. Effect of K_m on edge moment at 0.64 *psi* pressure; (1 *lb* = 4.45 *N*; 1 *in* = 2.54 *cm*).

Figure (7) shows the variation of the edge moment at $K_m=10^8$ ***lb/rad*** (4.45 x10^8 ***N/rad***) due to increasing pressures. As would be expected, the edge moment increases with the increase of the applied pressure, however this increase is not linear as would be predicted by linear solutions.

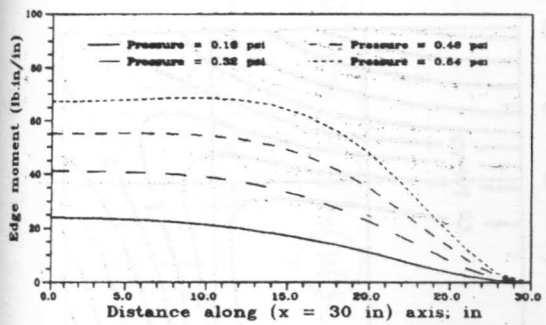

Figure 7. Effect of pressure on edge moment at $K_m = 10^8$ *lb*/rad; (1 *IB* = 4.45 *N*; 1 *psi* = 6.9 *kPa*).

The effects of changes in the bending stiffness K_m on the principal stresses under lateral pressure of 0.64 ***psi*** (4.41 *kPa*) are reported in Figure (8). Contour lines for maximum principal stress for K_m = 0.0 ; 10^2 ; 10^3 ; and 10^8 ***lb/rad*** are presented in Figures. (8-a to 8-d). Also maximum principal tensile stresses are summarized in Table (1). It was found that as the glass plate becomes more constrained, the maximum principal tensile stress decreases rapidly. Also, with the increase of K_m the area of the maximum principal tensile stress is increased and moves inward towards the plate center (see Figure 8).

Table 2 reports the number of iterations required in the numerical solution to achieve convergence at an iteration tolerance of 0.001. As can be seen from this table, and with the exception of cases 1 and 2 where the plate is subjected to very small pressures, the number of iterations decrease with the increase of the value of K_m. This can be explained by the fact that as the value of K_m increases the plate becomes more constrained and hence the number of degrees of freedom become less.

CONCLUSIONS

The following conclusions are reached from the finite difference model for the nonlinear analysis of glass plates resting on elastic supports, which offer both rotational and out-of-plane restraints.

1- It is shown that the finite difference model presented in this study can be a useful model to calculate nonlinear stresses and deformations of thin rectangular plates resting on elastic supports.
2- The maximum principal tensile stress decreases rapidly with the increase of the value of the spring constant of the bending restraints (K_m).
3- With the increase in the value of K_m, The area of the maximum principal tensile stress increases and moves inward towards the plate center.
4- For K_m = 10^3 ***lb/rad*** (4.45 x 10^3 ***N/rad***) the maximum deflection at pressure = 0.64 ***psi*** (4.41 ***kPa***) reduces to 80% of the corresponding deflection of a simply supported plate 60x60x0.1875 ***in*** (152.4x152.4x0.48 *cm*).
5- The difference of changes in K_m on plate stresses and deformations is negligible for values of K_m exceeding about 10^5 ***lb/rad*** (4.45x10^5 ***N/rad***) for the above mentioned glass plate.
6- The number of iterations required in the numerical solution decrease with the increase in the value of K_m.

ACKNOWLEDGMENTS

The research described in this paper was performed in the Civil Engineering Department at Texas Tech University between November, 1991 and April 1992. The financial support received from the Egyptian Government and the USA through the Peace Fellowship Program is gratefully acknowledge. The writer wishes to thank Prof. C.V.G. Vallabhan of Texas Tech University for his helpful suggestions and constructive criticism.

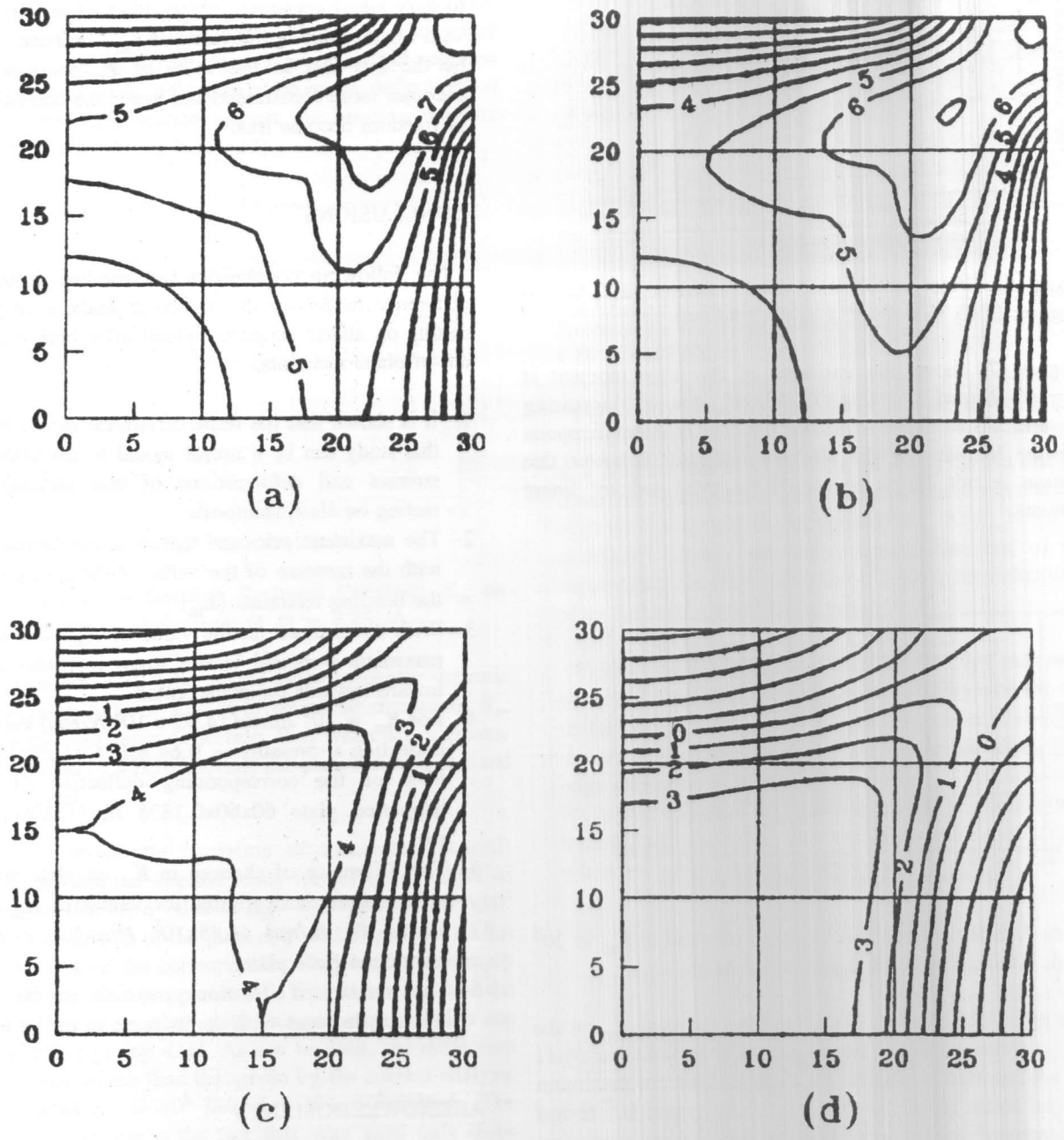

Figure 8: Effect of bending stiffness K_m on maximum principal stresses at pressure = 0.64 *psi* (principal stresses are in *ksi*); (1 *in* = 2.54 *cm*; 1 *psi* = 6.9 *kPa*; 1 *lb* = 4.45 *N*). (a) $K_m = 0$; (b) $K_m = 10^2$ *lb/rad*; (c) $K_m = 10^3$ *lb/rad*; (d) $K_m = 10^8$ *lb/rad*.

APPENDIX I. FINITE DIFFERENCE MOLECULES

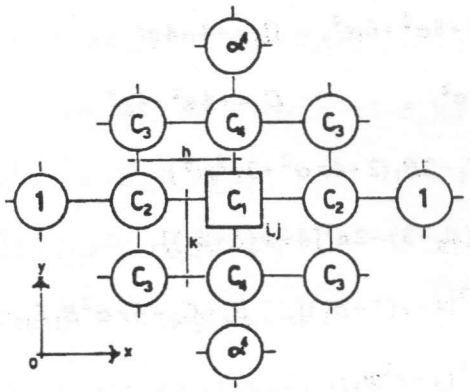

$$\nabla^4 w_{i,j} = \textit{shown Molecule} = \frac{h^4}{D} q_{i,j}$$

Figure 9. Finite difference molecule for ∇^4 for all interior nodes.

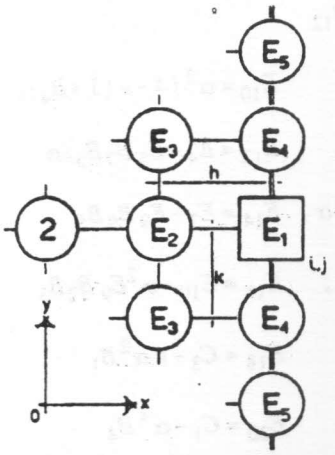

$$\nabla^4 w_{i,j} = \textit{shown Molecule} = \frac{h^4}{D} q_{i,j} + \frac{2h^3}{D} V_{i,j}$$

Figure 10. Finite difference molecule for ∇^4 at the edge $x = a/2$.

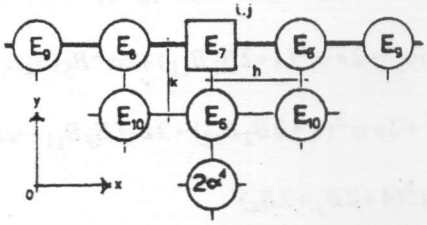

$$\nabla^4 w_{i,j} = \textit{shown Molecule} = \frac{h^4}{D} q_{i,j} + \frac{2\alpha h^3}{D} V_{i,j}$$

Figure 11. Finite difference molecule for ∇^4 at the edge $y = b/2$.

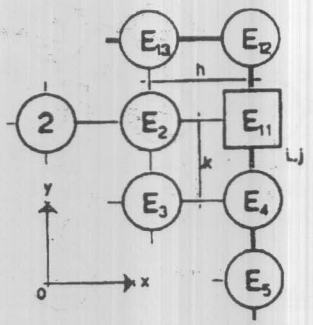

$$\nabla^4 w_{i,j} = \textit{shown Molecule} = \frac{h^4}{D} q_{i,j} + \frac{2h^3}{D} V_{i,j}$$

Figure 12. Finite difference molecule for ∇^4 at $x = a/2$ (near the corner).

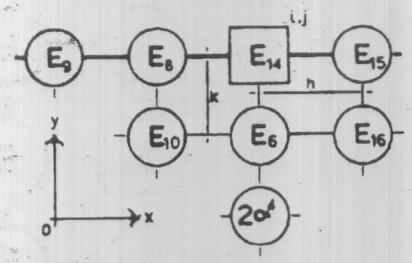

$$\nabla^4 w_{i,j} = \textit{shown Molecule} = \frac{h^4}{D} q_{i,j} + \frac{2\alpha h^3}{D} V_{i,j}$$

Figure 13. Finite difference molecule for ∇^4 at $y = b/2$ (near the corner).

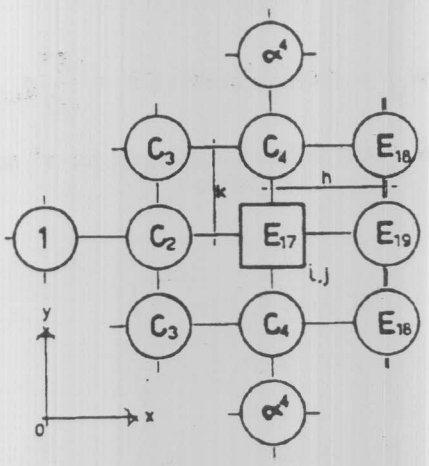

$$\nabla^4 w_{i,j} = \textit{shown Molecule} = \frac{h^4}{D} q_{i,j}$$

Figure 14. Finite difference molecule for ∇^4 near the edge $x = a/2$.

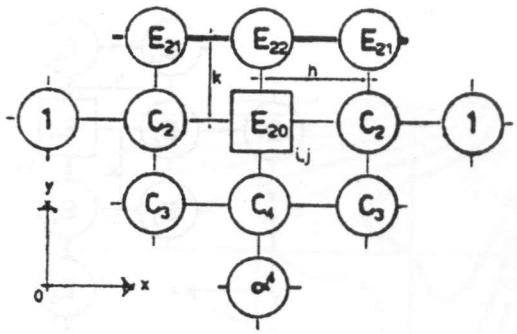

$$\nabla^4 w_{i,j} = \textit{shown Molecule} = \frac{h^4}{D} q_{i,j}$$

Figure 15. Finite difference molecule for ∇^4 near the edge $y = b/2$.

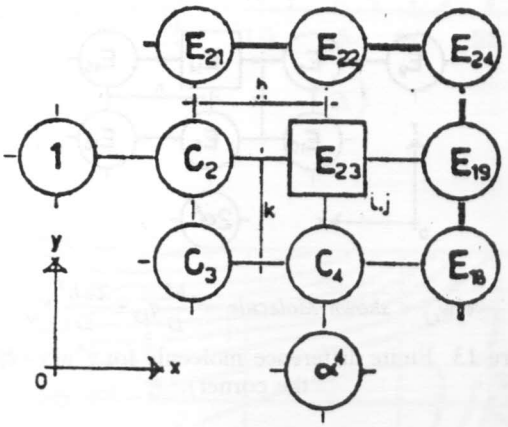

$$\nabla^4 w_{i,j} = \textit{shown Molecule} = \frac{h^4}{D} q_{i,j}$$

Figure 16. Finite difference molecule for ∇^4 near plate edges.

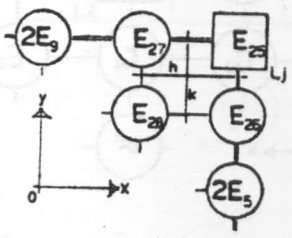

$$\nabla^4 w_{i,j} = \textit{shown Molecule} = \frac{h^4}{D} q_{i,j} + \frac{2h^3}{D}(1+\alpha) V_{i,j} + \frac{4\alpha h^2}{D(1-\nu)} R_{i,j}$$

Figure 17. Finite difference molecule for ∇^4 at the corner of the plate.

In the above Figures (Figures (9-17)) we have:

$C_1 = 6 + 8\alpha^2 + 6\alpha^4$, $C_2 = -4 - 4\alpha^2$

$C_3 = 2\alpha^2$, $C_4 = -4\alpha^2 - 4\alpha^4$

$E_1 = C_1 - 2B_1(2 + 4\nu\alpha^2 + 3\nu^2\alpha^4)$,

$E_2 = 2(B_3 - 3) - 2\alpha^2[4 - \nu(1 + B_3)]$,

$E_3 = \alpha^2[4 - \nu(1 + B_3)]$, $E_4 = C_4 + 4\nu\alpha^2 B_1 B_{11}$

$E_5 = \alpha^4(1 - \nu^2 B_1)$,

$E_6 = -8\alpha^2 - 2\alpha^4(3 - B_4) + 2\nu\alpha^2(1 + B_4)$

$E_7 = C_1 - 2\alpha^2 B_2(2\alpha^4 + 4\nu\alpha^2 + 3\nu^2)$,

$E_8 = C_2 + 4\nu\alpha^2 B_2 B_{12}$

$E_9 = 1 - \nu^2\alpha^2 B_2$, $E_{10} = \alpha^2[4 - \nu(1 + B_4)]$

$E_{11} = E_1 - E_5 B_6 B_5$, $E_{12} = E_4 - E_5 B_7 B_5/\alpha$

$E_{13} = E_3 - E_5 B_8 B_5/\alpha$, $E_{14} = E_7 - E_9 B_9 B_5$

$E_{15} = E_8 - E_9 B_{10} B_5$, $E_{16} = E_{10} - \alpha^2 E_9 B_8 B_5$

$E_{17} = C_1 - B_3$, $E_{18} = C_3 - \nu\alpha^2 B_1$

$E_{19} = C_2 - 2B_1 B_{11}$, $E_{20} = C_1 - \alpha^4 B_4$

$E_{21} = C_3 - \nu\alpha^4 B_2$, $E_{22} = C_4 + 2\alpha^4 B_2 B_{12}$

$E_{23} = E_{20} - B_3$, $E_{24} = E_{21} - \nu\alpha^2 B_1$

$E_{25} = C_1 - 2\nu^2\alpha^2(\alpha^2 B_1 + B_2) + 2B_5(B_{10} B_{11} + \alpha B_7 B_{12})$

$E_{26} = -8\alpha^2 - 6\alpha^4 + 2\nu\alpha^2(1 + 2B_1 B_{11}) + 2\alpha^2 B_5(B_8 B_{11} +$

$E_{27} = -6 - 8\alpha^2 + 2\nu\alpha^2(1 + 2B_2 B_{12}) + 2B_5(B_9 B_{11} + \alpha B_8$

$E_{28} = 8\alpha^2 - \nu\alpha^2(4 + 2B_3 + 2B_4)$

Where:

$\alpha = h/k$ = aspect ratio of the finite difference grid.

$V_{i,j} = -K_v w_{i,j}$, $R_{i,j} = 2D(1-\nu)(w_{,xy})_{i,j}$

$B_o = -K_m h/(2D)$, $B_1 = 1/(1-B_o)$

$B_2 = 1/(\alpha^2 - \alpha B_o)$, $B_3 = (1+B_o)B_1$

$B_4 = (\alpha^2 + \alpha B_o)B_2$, $B_5 = 1/[\nu^2\alpha - (1-B_o)(\alpha - B_o)]$

$B_6 = \nu^2\alpha - (\alpha + B_o)(1 - B_o)$,

$B_7 = 2\alpha^2(1-\nu^2) - 2B_o(\nu + \alpha^2)$

$B_8 = 2\nu B_o$, $B_9 = \nu^2\alpha - (1+B_o)(\alpha - B_o)$

$B_{10} = 2\alpha(1-\nu^2) - 2B_o(1+\nu\alpha^2)$,

$B_{11} = 1 + \nu\alpha^2$

$B_{12} = \alpha^2 + \nu$

REFERENCES

[1] Timoshenko, S., and Woinowsky-Krieger, S., "Theory of Plates and Shells," McGraw-Hill Company, Inc., New York, 1965.

[2] Al-Tayyib, A-H., "Geometrically Nonlinear Analysis of Rectangular Glass Panels by Finite Element Method," Ph.D. Dissertation, Texas Tech University, 1980.

[3] Tsai, C.R., and Stewart, R.A., "Stress Analysis of Large Deflection of Glass plates by Finite Element Method," Journal of American Ceramic Society, Vol. 59, Nos. 9-10, 1976, pp. 445-448.

[4] Vallabhan, C.V.G., "Iterative Analysis of Nonlinear Glass Plates," Journal of Structural Engineering, ASCE, Vol. 109, No. 2, Feb., 1983.

[5] Wang, B.Y-T., "Nonlinear Analysis of Rectangular Glass Plates by Finite Difference Method," M.Sc. Thesis, Texas Tech University, 1981.

[6] Szilard, R., "Theory and Analysis of Plates - Classical and Numerical Methods," Prentice-Hall, Inc., Englewood Cliffs, N.J., 1974.

[7] Fung, Y.C., "Foundations of Solid Mechanics," Prentice-Hall, Inc. Englewood Cliffs, N.J., 1965.